MOLECULAR AND CELLULAR BIOLOGY, Feb. 2008, p. 1018–1028 Vol. 28, No. 3
0270-7306/08/$08.00+0 doi:10.1128/MCB.01136-07

Inactivation of the Polycomb Group Protein Ring1B Unveils an Antiproliferative Role in Hematopoietic Cell Expansion and Cooperation with Tumorigenesis Associated with *Ink4a* Deletion▽†

Carmela Calés,[2] Mónica Román-Trufero,[1] Leticia Pavón,[2] Iván Serrano,[2] Teresa Melgar,[1] Mitsuhiro Endoh,[3] Claudia Pérez,[4] Haruhiko Koseki,[3] and Miguel Vidal[1,3]*

Centro de Investigaciones Biológicas, Consejo Superior de Investigaciones Científicas, Ramiro de Maeztu 9, 28004 Madrid, Spain[1]; Instituto de Investigaciones Biomédicas, Universidad Autónoma de Madrid, Consejo Superior de Investigaciones Científicas, Arturo Duperier 4, 28029 Madrid, Spain[2]; Riken Research Center for Allergy and Immunology, 1-7-22 Suehiro, Tsurumi-ku, Yokohama 230-0045, Japan[3]; and Anatomy and Histopathology, Facultad de Veterinaria, Universidad de León, Campus Vegazana, 24071 León, Spain[4]

Received 26 June 2007/Returned for modification 2 August 2007/Accepted 12 November 2007

Polycomb group (PcG) proteins act as positive regulators of cell proliferation. *Ring1B* is a PcG gene essential for embryonic development, but its contribution to cell turnover in regenerating tissues in not known. Here, we have generated a conditional mouse mutant line to study the Ring1B role in adult hematopoiesis. Mutant mice developed a hypocellular bone marrow that paradoxically contained an enlarged, hyperproliferating compartment of immature cells, with an intact differentiation potential. These alterations were associated with differential upregulation of cyclin D2, which occurred in all mutant bone marrow cells, and of $p16^{Ink4a}$, observed only in the differentiated compartment. Concurrent inactivation of *Ink4a* rescued the defective proliferation of maturing cells but did not affect the hyperproliferative activity of progenitors and resulted in a shortening of the onset of lymphomas induced by *Ink4a* inactivation. These data show that Ring1B restricts the progenitors' proliferation and promotes the proliferation of their maturing progeny by selectively altering the expression pattern of cell cycle regulators along hematopoietic differentiation. The novel antiproliferative role of Ring1B's downregulation of a cell cycle activator may play an important role in the tight control of hematopoietic cell turnover.

Adult multicellular organisms have evolved cell turnover strategies adapted to the maintenance and repair of tissues. In many cases, such as the hematopoietic system, gut, skin, and brain, tissue homeostasis depends on the activity of multipotent stem cells from which derive all the cell lineages that make these tissues (17, 56). Because of the relatively small number of stem cells, their progeny undergoes an expanding but limited number of cell divisions along the differentiation process before entering the mitotically inactive state of fully mature cells. Tissue homeostasis, then, depends on an adequate balance between stem cell renewal, regulated cell proliferation, and terminal differentiation of stem cell progeny (58, 74).

The Polycomb group (PcG) of proteins are transcriptional repressors that prevent the inappropriate expression of genes that determine cell identity (4, 11). PcG gene products assemble in multimeric complexes (Polycomb repressing complexes [PRC]) whose transcriptional activity is associated to their role as chromatin modifiers (64). PRC are compositionally diverse, but depending on which of two sets of core subunits they contain, they are designated type PRC1 or PRC2 (40). Histone H2AK119 monoubiquitylation depends on the RING finger E3 ligases of PRC1 complexes (10, 73), whereas histone H3K27 trimethylation is carried out by PRC2 complexes (12, 18, 34, 46). Well known as developmental regulators (57), PcG genes also play important roles in cell proliferation control (41, 52). Murine models of loss of function of PcG genes encoding PRC1 subunits show reduced size and hypocellularity of hematopoietic organs (1, 15, 69, 70) and also, in some cases (Bmi1) of brain structures (71), indicating that PcG complexes are positive regulators of cell proliferation. The upregulation of PcG products observed in a wide variety of tumors (54, 68) and their cooperation in oncogene-induced tumorigenesis (27) further support a role for PcG complexes as promoters of proliferation. Exceptionally, inactivation of the PRC2 subunit Eed resulted in enlarged hematopoietic compartments (36). These alterations are due, at least in part, to PcG-mediated repression of the *Ink4a*/*Cdkn2a* locus, which encodes the tumor suppressors $p16^{Ink4a}$ and $p19^{Arf}$. Loss of function of PRC1 proteins, and Bmi1 in particular, results in premature senescence of hematopoietic and neuronal stem cells (28, 37, 44, 48, 49, 51). PcG complexes also promote expansion of maturing cells by preventing senescence and apoptosis, although the contribution of each of these mechanisms varies depending on the particular tissue and the PcG protein (9, 14, 38, 45).

Ring1B and its paralog Ring1A are the RING finger E3 ligases that monoubiquitylate H2A (20, 73). They associate directly with Bmi1, Mel18, M33, and Phc1, forming the core of

* Corresponding author. Mailing address: Developmental and Cell Biology, Centro de Investigaciones Biológicas, Ramiro de Maeztu, 9, 28040 Madrid, Spain. Phone: 34 91 837 3112, ext. 4383. Fax: 34 91536 0432. E-mail: mvidal@cib.csic.es.

† Supplemental material for this article may be found at http://mcb.asm.org/.

▽ Published ahead of print on 26 November 2007.

PRC1 complex(es) (25, 39, 63). The contribution of Ring1A and Ring1B to cell turnover of renewing tissues is not known. Constitutive inactivation of Ring1A results in fertile mice with no overt phenotypes (19), whereas inactivation of Ring1B leads to embryonic lethality due to defective gastrulation (72). Considering that Ring1B expression in the adult hematopoietic compartment is detected in all differentiation stages, from the hematopoietic stem cells (HSCs) and their immature descendants (29), we sought to address the role of Ring1B in adult hematopoiesis using a conditional mutant mouse line. We find that Ring1B inactivation results in a reduction of total bone marrow cells and, at the same time, an enlargement of the immature cell compartment. We also show that the alterations in the size of bone marrow cell populations are due to cell proliferation defects caused by upregulation of components of the cell cycle machinery that act as activators (cyclin D2) or inhibitors ($p16^{Ink4a}$) of proliferation in a differentiation stage-dependent manner. Finally, we observed premature development of lymphomas in compound *Ring1B*;*Ink4a* mutant mice that suggests an important role for Ring1B in controlling the expansion of progenitor cells in adult hematopoiesis.

MATERIALS AND METHODS

Mice, genotyping, and conditional inactivation of *Ring1B*. *Ring1B* genomic sequences for the targeting vector were generated from a partial genomic clone isolated from a mouse 129SVJ Lambda FIX II phage library (Stratagene) probed with a *Ring1B* cDNA. The 5′ arm of the targeting vector was a 4,680-kb EcoRI-BstNI fragment corresponding to sequences located 4,464 bp 5′ from the intron 2-exon 3 junction, and the 3′ arm was a 5,286-bp BstNI-EcoRI fragment encompassing sequences up to 97 bp 3′ of the exon 5-intron 5 boundary. They were subcloned into pPGKneo2loxDTA plasmid (67), which contains a phosphoglycerol kinase promoter-*neomycin* resistance gene cassette flanked by two *loxP* sites and a phosphoglycerol kinase-*diphteria toxin* gene cassette (see Fig. S1A in the supplemental material). The 5′ arm was modified by inserting an oligonucleotide containing a *loxP* sequence and a BglII site at the AvrII site 197 bp 5′ from the intron 1-exon 2 junction using a PCR strategy. The targeting construct was linearized and electroporated into 2×10^7 mouse R1 embryonic stem (ES) cells. Colonies surviving the G418 selection were transferred into duplicated 48-well plates, which were used to prepare frozen stocks of the ES cell colonies and to isolate genomic DNA, respectively. The targeted allele was identified by Southern blotting using probes external to the targeting vector (see Fig. S1A in the supplemental material). Two $Ring1B^{flox/+}$ (hereafter, $Ring1B^{f/+}$) ES clones were aggregated with morulae obtained from C57Bl10 mice, and the resulting chimeric males were mated to C57Bl10 mice, and heterozygous animals were identified by Southern blotting. For routine genotyping, genomic DNA was analyzed by using a three-primer PCR (see Fig. S1A in the supplemental material).

For in vivo conditional inactivation, $Ring1B^{flox/flox}$ (hereafter, $Ring1B^{f/f}$) mice were crossed with *MxCre* transgenic mice (33). *MxCre* expression was induced by intraperitoneally injecting 250 μg of polyinosine-polycytidine (pIpC; Pharmacia) on three alternate days in 6- to 12-week-old mice. "Ex vivo" conditional inactivation of *Ring1B* was carried out on cells obtained from mice generated by crossing $Ring1B^{f/f}$ mice with $RERT^{ert}$ mice, a mouse line in which an *IRES-Cre-ERT2* (tamoxifen-inducible Cre) cassette was knocked in into the 3′ untranslated region of the RNA *polII* (*Polr2a*) gene (43), to obtain $Ring1B^{f/f}$; $RERT^{ert/ert}$ mice (here termed $Ring1B^{f/f}$ *CreERT2*). Translocation of Cre-ERT2 to cell nuclei and *loxP* recombination were achieved by adding to the cultures 4′-hydroxy tamoxifen ([4-HT] 0.4 μM final concentration; Sigma) or vehicle (+4-HT and −4-HT cultures, respectively).

Compound $Ring1B^{fl/fl}$; $Ink4a^{-/-}$ mice were obtained by crossing $Ring1B^{f/f}$ mice with the $Ink4a^{-/-}$ mouse line (65). Genotyping of the *Ink4a* allele was done by Southern blotting as described previously (65). All mouse procedures were institutionally approved and were in accordance with national and European regulations.

Cell counting and blood analysis. Bone marrow cells were flushed out of both femurs with phosphate-buffered saline (PBS) containing 2% fetal calf serum (PBS–2% FCS) under sterile conditions. Spleens and thymi were disrupted in a Dounce homogenizer (loose pestle) in PBS–2% FCS. Cells were counted in a hemocytometer.

Blood was obtained by heart puncture immediately after mice were sacrificed. Blood counts were mostly performed by manual counting on a hemocytometer or automatically using an Abacus (Diatron) hematological analyzer. Manual counting of white blood cells was carried out after erythrocytic lysis.

Immunophenotyping and cell separation. Single-cell suspensions were washed with PBS and resuspended in cold washing solution (PBS–2% FCS–0.1% sodium azide). The appropriate antibodies were then added, and cells were labeled for 20 min at 4°C. After a washing step, cells labeled with biotin-conjugated antibodies were further incubated with streptavidin conjugated to phycoerythrin (PE) or peridinin chlorophyll protein-Cy5.5. Samples were acquired in a FACScan fluorescence-activated cell sorter (FACS) instrument with CellQuest software or a FACSCanto with Diva software, all from Becton Dickinson. The antibodies that were used were as follows: c-Kit conjugated to fluorescein isothiocyanate (FITC), biotin, or allophycocyanin (for analysis); Sca-1, Gr-1, CD41, and B220 conjugated to FITC or biotin; Mac-1, CD3, and Ter119 conjugated to biotin; CD34 conjugated to FITC; FcγR and CD19 conjugated to PE. All antibodies were purchased from BD Biosciences.

For common myeloid progenitor (CMP) sorting, isolated colonies with immature phenotype were pooled, immunomagnetically depleted of Lin^+ cells, and labeled with anti-c-Kit-allophycocyanin -, anti-CD34-FITC-, and anti-FcγR-PE-conjugated antibodies and sorted on the c-Kit^+/$CD34^+$/$Fc\gamma R^{lo}$ gate in a FACS Vantage sorter equipped with a Diva system (BD Biosciences), set to render the highest purity. Immunomagnetic cell isolation was done using a Lineage Cell Depletion kit and LD columns together with a QuadroMACS separation unit from Miltenyi Biotec. Hematopoietic cell subpopulations for Ring1B expression analysis were isolated by cell sorting as described previously (30), using $Mac1^+$ $Gr1^{lo}$ for monocytic and $Mac1^+$ $Gr1^{high}$ for granulocytic precursors, respectively, in a FACS Vantage sorter (BD Biosciences).

In vitro colony forming assays. Myeloid and pre-B-cell colony plating assays were performed in cytokine-supplemented methylcellulose-based medium M3434 and M3630 (StemCell Technologies), seeding total bone marrow in duplicate (2×10^5 or 2×10^4 cells/35-mm dish for pre-B-cell and myeloid assays, respectively). For assays of isolated progenitors, 500 Lin^- cells were used per plate. Myeloid cultures were scored for colony formation and morphologically analyzed at day +12 unless otherwise specified. Pre-B-cell and immature myeloid colonies were systematically scored at day +8 and day +7 after seeding, respectively. Serial replating, using equal numbers of cells, was performed 10 days after plating.

Cell proliferation, cell division, and apoptosis assays. Bone marrow or isolated Lin^- cells were cultured in 24-well plates containing Iscove's modified Dulbecco's medium–10% FCS medium plus 20 or 50 ng/ml of recombinant murine interleukin-3 (IL-3) or recombinant human IL-6, respectively (Peprotech). Recombination in cultured cells was achieved by adding 4-HT (0.4 μM; Sigma) or vehicle, where indicated. Lin^- cells cultures also contained 100 ng/ml of recombinant human stem cell factor (Peprotech). Viable cells were counted by trypan blue exclusion in a hemocytometer.

Bromodeoxyuridine (BrdU) incorporation was assessed by adding the nucleotide precursor analog to the culture medium at a final concentration of 10 μM. After 18 h labeled cells were determined with a flluorochrome-conjugated anti-BrdU antibody (FITC BrdU flow kit; BD-Pharmingen) and analyzed by flow cytometry in a FACScan cytometer equipped with CellQuest software (BD Biosciences). For cell division assays, cells were labeled with 2 μM carboxyfluorescein diacetate succinimidyl ester (CFDA-SE) and handled as indicated by the manufacturer (Invitrogen). Cell-associated fluorescence was analyzed by flow cytometry 18 h later. To determine the fluorescence associated to cells before division, two aliquots were removed: one was analyzed immediately, and the second was kept at 4°C to match the analysis conditions. An FITC-conjugated recombinant human annexin V kit (Bender Medsystems) was used to stain apoptotic cells prior to flow cytometry analysis.

Western blotting analysis. Cells were lysed in radioimmunoprecipitation assay buffer (10 mM Tris-HCl, pH 7.2, 150 mM NaCl, 1% TX-100, 0.1% sodium dodecyl sulfate, 1% deoxycholate, 5 mM EDTA, 20 mM NaF, 100 μM orthovanadate, and protease inhibitors) for 30 min on ice. Cell lysates were cleared of debris by centrifugation at 15,000 × *g* for 15 min, aliquoted, snap-frozen, and kept at −70°C until used. Thirty micrograms of total protein was subjected to sodium dodecyl sulfate-polyacrylamide gel electrophoresis and transferred to BioTrace polyvinylidene difluoride membranes (Pall Corporation) for 1 h at 2 mA/cm^2 on a semidry transfer apparatus (Amersham). Ponceau staining was routinely performed on membranes, and digital photographs were taken in order to record a sample loading control. After being blocked in Tris-buffered saline containing 0.1% Tween 20 and 5% nonfat dry milk, filters were incubated

overnight at 4°C with the following antibodies: anti-Ring1B (63), anti-$p16^{Ink4a}$ (M-156; Santa Cruz), anti-cyclin D2 (M-20; Santa Cruz), anti-cyclin D3 (C-16; Santa Cruz), anti-$p27^{kip1}$ (clone 57; Transduction Laboratories), anti-cdc6 (Ab-3; Oncogene), anti-$p57^{kip2}$ (KP-39; Sigma), anti-cyclin A (H-432; Santa Cruz), anti $p19^{Arf}$ (ab80; Abcam). After a washing step and incubation with horseradish peroxidase-conjugated secondary antibodies (Dako), signals were detected using an enhanced chemiluminescence system (Pierce).

Histopathology and immunohistochemistry. Normal and tumor tissue samples were fixed in 10% neutral-buffered formalin for 24 h. After dehydration and paraffin wax embedding, 3-μm sections were prepared and stained with hematoxylin and eosin. For immunohistochemical analysis, sections were mounted on poly-L-lysine-coated slides, and anti-Pax5 antibodies were detected by the avidin-biotin-peroxidase complex method (Peroxidase Elite, Vectastain, and ABC kit; Vector Laboratories).

Quantitative reverse transcription-PCR expression analysis. RNA was isolated from sorted hematopoietic cell populations using an RNeasy kit (Qiagen). Random-primed cDNA was generated using a Superscript III First Strand reverse transcription kit (Invitrogen). Triplicate reactions of cDNA amplification were performed in Sybr Premix Ex *Taq* (Takara) and analyzed using a 7900HT Fast Real-Time PCR System (Applied Biosystems). Relative mRNA normalized to acidic ribosomal phosphoprotein mRNA levels was determined using the comparative cycle threshold ($\Delta\Delta C_T$) method. The following sets of primers were used: for Ring1B, TTGACATAGAATGGGACAGC (forward) and GTCAGC AGAAAGTCTTGTGG (reverse); for acidic ribosomal phosphoprotein, CGAC CTGGAAGTCCAACTAC (forward) and ATCTGCTGCATCTGCTTG (reverse).

ChIP. Lin^- and Lin^+ bone marrow cells were processed for chromatin immunoprecipitation (ChIP) assays using anti-trimethylated H3K27 (Upstate), anti-Ring1B (3), and anti-Bmi1 (21) antibodies. Immunoprecipitated DNA was amplified using the primer pair TTGCCCTGAATATAGCATGA and TCATG CTATATTCAGGGCAA or the pair CGATCCTTTAGCGCTGTTTC and CA CACTCTGCTCCTGACCTG that span 271 bp and 201 bp in the murine $p16^{Ink4a}$ gene promoter area, respectively.

Statistical analyses. Values are expressed as means ± standard deviation (SD). Data sets were compared using a two-tailed Student's *t* test, and differences were considered significant for *P* values of <0.05.

RESULTS

Loss of *Ring1B* leads to concurrent bone marrow hypocellularity and enlarged immature cell compartments. Ring1B mRNA expression was found to be ubiquitous in hematopoietic cells, from the most primitive HSC and its derived progenitors (CMP and common lymphoid progenitor) through more committed but still immature bivalent progenitors (granulo-monocytic progenitors [GMPs] and megakaryo-erythrocytic progenitors [MEP]) and the most mature myeloid and lymphoid cells (Fig. 1A). To study the function of Ring1B during adult hematopoiesis, we crossed a pIpC-inducible MxCre mouse line that expresses the Cre recombinase in the hematopoietic compartment (33) with a conditional *Ring1B*$^{f/f}$ mouse line (Fig. 1B) to produce *Ring1B*$^{f/f}$; *MxCre* mice and their *MxCre*-negative littermate controls. Six- to 12-week-old mice were treated with pIpC and sacrificed 4 weeks later. The treatment resulted in efficient deletion of alleles flanked by *loxP* sites (see Fig. S1A in the supplemental material) and loss of Ring1B protein in the bone marrow (Fig. 1B).

Examination of circulating blood cells and secondary hematopoietic organs (spleen and thymus) of *MxCre*-positive and *MxCre*-negative mice showed only mild, but consistent, reduction of erythrocytes and splenocytes in most mutant animals and a few thrombocytotic individuals (see Fig. S2A and B in the supplemental material). Immunophenotypic analysis of bone marrow cells showed no remarkable differences in lineage composition between normal and mutant mice, except for a slight decrease of mutant lymphoid B cells (see Fig. S2C in the supplemental material). A relevant difference, however, was seen in total bone marrow cell numbers, which were reduced upon *Ring1B* ablation by nearly one-third ($P = 0.001$) (Fig. 1C). In contrast, the progenitor compartment (minority cells lacking lineage differentiation markers, i.e., Lin^- cells) was enlarged in mutant bone marrow (Fig. 1D). The HSC-enriched subpopulation (Lin^- cells that simultaneously express c-Kit and Sca-1 markers) was also larger than that of Ring1B-expressing cells (Fig. 1E). Thus, *Ring1B* ablation resulted in concurrent hypocellularity of the mature bone marrow and an increased number of progenitor cells, with no apparent alterations in lineage specification.

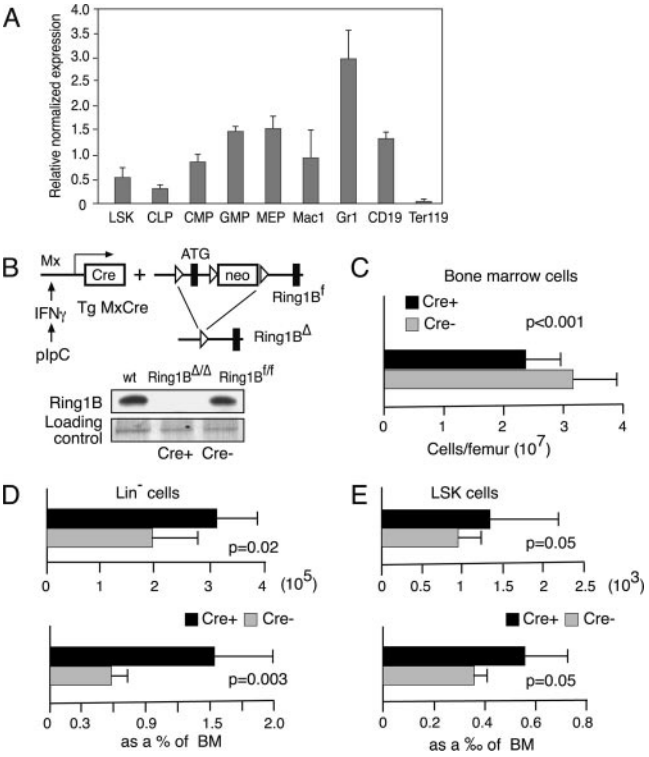

FIG. 1. Conditional targeting of *Ring1B* and analysis of *Ring1B*-deficient bone marrow cells. (A) Analysis by quantitative reverse transcription-PCR of the expression levels of Ring1B in the indicated subpopulations of hematopoietic progenitors and their maturing progeny. LSK, $Lin^-Sca\text{-}1^+c\text{-}Kit^+$ cells, corresponding to long- and short-term HSCs; CLP, common lymphoid progenitors; Mac1, monocytic precursors; Gr1, granulocytic precursors; CD19, B-cell precursors; Ter119, erythocytic precursors. Each value has been normalized for acidic ribosomal phosphoprotein expression levels. (B) Schematic representation of strategy used to ablate *Ring1B* in vivo and results of Ring1B detection by Western blotting in bone marrow from *Ring1B*$^{f/f}$ mice and from mice lacking the *Ring1B* locus (*Ring1B*$^{\Delta/\Delta}$). (C) Total bone marrow cell count from *Ring1B*$^{f/f}$ ($n = 20$; Cre^-) and *Ring1B*$^{\Delta/\Delta}$ ($n = 20$; Cre^+) mice. (D) Absolute (top) and relative (bottom) numbers of bone marrow cells lacking lineage markers (Lin^- population, corresponding to HSC and all progenitor cells) from *Ring1B*$^{f/f}$ ($n = 12$; Cre^-) and *Ring1B*$^{\Delta/\Delta}$ ($n = 12$; Cre^+) mice. (E) Absolute (top) and relative (bottom) numbers of LSK population (corresponding to long- and short-term HSCs) from control ($n = 10$; Cre^-) and mutant ($n = 10$; Cre^+) immunomagnetically isolated Lin^- cells. BM, bone marrow; IFN-γ, gamma interferon; wt, wild type; Tg, transgenic.

Cell-autonomous increase of *Ring1B*-deficient myeloid clonogenic cells. Clonogenic assays were employed to determine

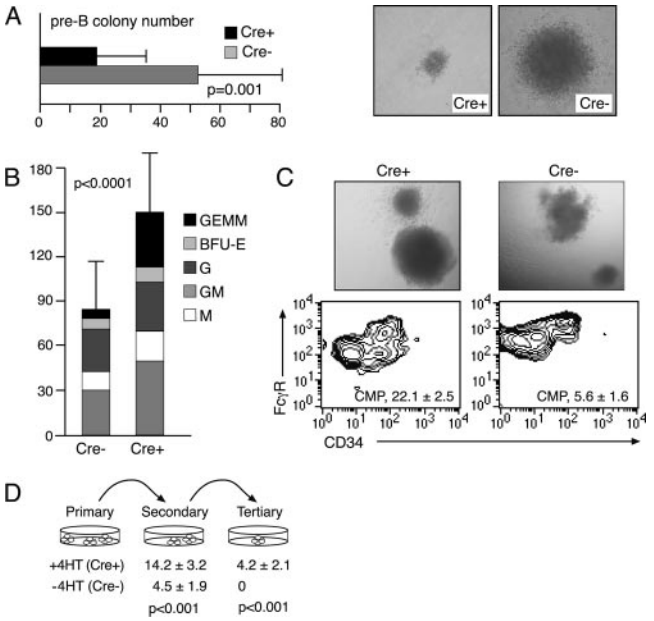

FIG. 2. Clonogenic assays of *Ring1B*-deficient bone marrow cells. (A) Impaired pre-B-cell colony formation in mice in which the *Ring1B* locus has been excised as a result of the expression of MxCre. Colonies generated per 5×10^5 bone marrow cells from mutant ($n = 14$; Cre^+) and control ($n = 12$; Cre^-) mice. At right are images of representative colonies at day +8 of culture. (B) Increased myeloid clonogenic activity in $MxCre^+$ (excised *Ring1B*) mice ($n = 14$; Cre^+) compared to $MxCre^-$ (nonexcised *Ring1B*) mice ($n = 16$; Cre^-). Bar segments represent the average absolute number (CFU) of the various colony types: unilineage monocytic (M), granulocytic(G), and erythrocytic (BFU-E) and bilineage granulo-monocytic (GM) and GEMM (mixed) colonies. (C) Myeloid colonies. At top are photographs of representative individual immature colonies picked at day +7 of culture; at bottom are contour plots of the flow cytometry analysis of these colonies showing the myeloid progenitors MEPs, GMPs, and CMPs identified as $CD34^-$ $Fc\gamma R^{lo}$ (lower left lobe), $CD34^+$ $Fc\gamma R^+$ (upper right lobe), and $CD34^+$ $Fc\gamma R^{lo}$ (lower right lobe; almost absent in control Cre^- colonies), respectively. A representative experiment (out of three) is shown, indicating the CMP relative content value ± SD. (D) Replicating assay of ex vivo *Ring1B*-excised bone marrow cells. The results are shown as the mean ± SD ($n = 6$) of the total number of secondary and tertiary colonies generated from identical numbers of pooled primary control (−4-HT) and mutant (+4-HT) myeloid colonies.

the abundance of cells (CFU) able to expand and give rise to differentiated progeny in vitro. These include primitive, multilineage progenitors and immediate unilineage precursors that give rise to characteristic, morphologically distinguishable colonies. For lymphoid cells, clonogenic assays in the presence of IL-7 revealed a severe reduction in the number and size of *Ring1B*-deficient pre-B-cell colonies (Fig. 2A). On the other hand, ablation of *Ring1B* resulted in an almost twofold increase of myeloid CFU (Fig. 2B). Whereas all types of supported CFU were represented, their relative proportions were altered, particularly the mixed granulo-mono-erythromegakaryocitic (GEMM) colonies (sixfold increase; $P < 0.0001$) (Fig. 2B) originated from the most immature progenitors. The GEMM colonies derived from blast-like cell clusters, which in mutant bone marrow cultures appeared invariably denser (Fig. 2C, top) and also contained a higher proportion of the primitive CMP (fivefold increase; $P = 0.05$) (Fig. 2C, bottom). We conclude that Ring1B clearly affected both the size and clonogenic activity of the progenitors' compartment.

Since extrinsic signals affect hematopoiesis, we aimed to determine the cell-autonomous contribution to the above alterations. To do this, we devised an ex vivo *Ring1B* inactivation system that used bone marrow cells from *Ring1B*$^{f/f}$; *Cre-ERT2* mice. These were obtained by crossing the conditional *Ring1B*$^{f/f}$ mouse line with a *RERT*^{ert} mouse deleter line (*Cre-ERT2*::*Polr2a* [43]) (see Fig. S3A in the supplemental material). The mouse deleter line ubiquitously expresses a tamoxifen (4-HT)-inducible fusion protein between the Cre recombinase and a mutated ligand binding domain of the human estrogen receptor. Bone marrow cells from these mice were cultured in parallel in the absence (Cre^-) and in the presence (Cre^+) of 4-HT to generate control and *Ring1B*-deleted cells, respectively. Efficient *Ring1B* ablation was achieved 2 days after 4-HT treatment (see Fig. S3B in the supplemental material). As seen above for in vivo *Ring1B*-inactivated bone marrow cells (Fig. 2A and B), 4-HT treatment resulted in a reduction of pre-B-cell colonies, an increase in total Lin^- cells, and a larger number of myeloid CFU (see Fig. S3C to E in the supplemental material). Consistent with this, mutant progenitors (+4-HT; Cre^+) yielded more secondary and tertiary colonies in a replicating assay than control progenitors (−4-HT; Cre^-), indicating a higher self-renewal rate of *Ring1B*-deficient cells (Fig. 2D). These results indicate that alteration of immature cell populations and of their clonogenic activities are mostly due to a cell-autonomous defect resulting from the ablation of *Ring1B*.

***Ring1B* inactivation enhances the proliferative rate of myeloid progenitors.** We used ex vivo inactivation of *Ring1B* to investigate whether differences in cell proliferation rate, apoptosis, or cell differentiation could account for the accumulation of *Ring1B*-deficient primitive hematopoietic cells. Pulse labeling of Lin^- cells with BrdU demonstrated that more cells incorporated BrdU in 4-HT-treated (Cre^+) than in nontreated (Cre^-) cultures (Fig. 3A). We also used CFDA-SE fluorescence decay as an additional test of the cell division rate. This assay is based on the dilution of the fluorescent dye resulting from its equal distribution among daughter cells upon cell division. As shown in Fig. 3B, nearly all *Ring1B*-deficient Lin^- cells had completed one cell cycle at the same point when 30% of the *Ring1B*-expressing Lin^- cells still remained undivided. Under these culture conditions, annexin V labeling (an indicator of apoptosis) showed no differences between treated and nontreated cultures (Fig. 3C). These results indicate that the enlargement of the mutant Lin^- compartment is due to an increase in the cell proliferation rate provoked by the loss of *Ring1B*.

Although the representation of the various lineages in bone marrow and circulating cells in *Ring1B* mutant mice suggested that no major alterations in differentiation were occurring, we further tested this by immunophenotyping cells generated in methylcellulose cultures of Lin^- cells. As seen in Fig. 3D, levels of Gr-1, Mac-1, and CD-41 lineage markers (specific for granulocytes, monocytes, and megakaryocytes, respectively) showed no differences between cultures from *Ring1B*-deleted and nondeleted Lin^- cells. Moreover, FACS-sorted mutant CMPs retained the ability to give rise in vitro to more mature progeny, MEPs and GMPs (Fig. 3E). Together, these data

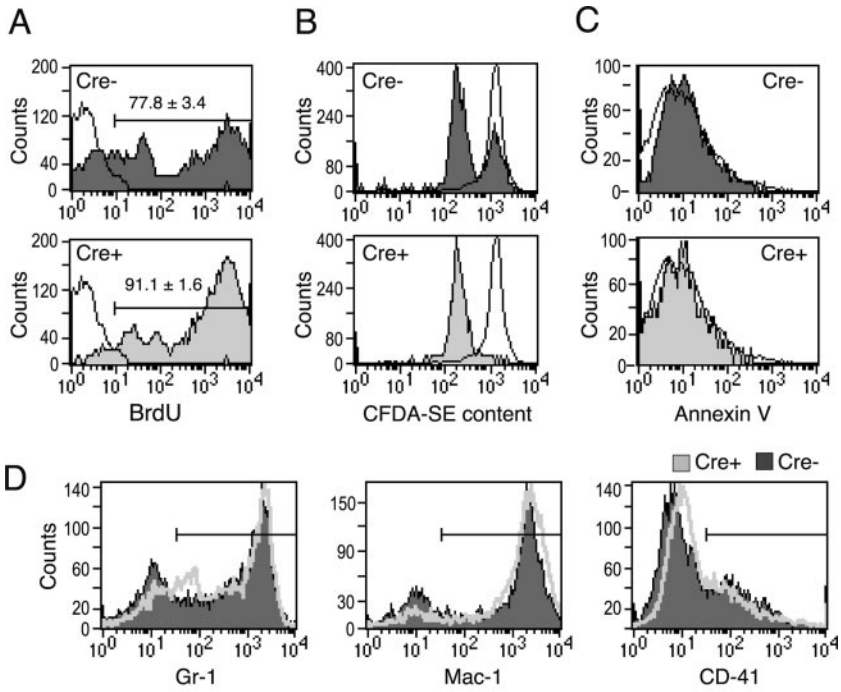

E

	Undifferentiated CMP (%)	Differentiated MEP + GMP (%)
Sorted CMP	>99.0	<1.0
d +7 myeloid differentiation (Exp. 1)	26.5	57.0
d +7 myeloid differentiation (Exp. 2)	36.2	53.8

FIG. 3. Increased proliferation of Ring1B-deficient progenitors. (A to C) Proliferation and apoptosis of Lin$^-$ cells isolated from *Ring1B$^{f/f}$*; *Cre-ERT2* bone marrow cells in the absence (Cre$^-$; top) or the presence (Cre$^+$; bottom) of 4-HT. (A) Solid plots correspond to cells labeled with anti-BrdU antibodies. Overlaid empty plots correspond to cells labeled with isotype-matching FITC antibody to define the BrdU-negative population. Proliferating, BrdU-positive cells (indicated by the bar) are shown as the mean ± SD of two duplicate, independent experiments. (B) CFDA-SE fluorescence content of mutant (+4-HT; Cre$^+$) (bottom) or control (−4-HT; Cre$^-$) (top) Lin$^-$ cells, 18 h after immunoseparation and fluorescent dye incubation. The empty histogram shows CFDA-SE cell content immediately after dye loading. (C) FITC-conjugated annexin V labeling of propidium iodide-impermeable viable Lin$^-$ cells cultured with (Cre$^+$; bottom) or without (Cre$^-$; top) 4-HT. The overlaid empty histogram corresponds to cells treated under the same conditions but with no added annexin V. (D) Expression of lineage markers in cells from mutant (light empty plots) and control (dark solid plots) myeloid colonies harvested at day +8. Gr-1, Mac-1, and CD41 markers stain mature cells of the granulocytic, monocytic, and megakaryocytic lineages, respectively. Bars indicate positively labeled cells. (E) Mutant CMPs retain their differentiation potential. Sorted mutant CMPs (Lin$^-$ c-Kit$^+$ CD34$^+$ FcγR^{lo}) cells were seeded into myeloid differentiation medium and individual colonies appearing at day +7 (d +7)were labeled with antibodies to c-Kit, CD34, and FcγR to determine MEP, CMP, and GMP content as indicated in the legend of Fig. 2.

strongly suggest that the accumulation of early progenitor cells resulting from *Ring1B* inactivation is mostly due to an enhanced proliferation rate of myeloid progenitors and not to reduced apoptosis or impairment of their differentiating ability.

Ring1B negatively regulates cyclin D2 and p16^{Ink4a}. After establishing the role of Ring1B in proliferation of hematopoietic cells, we began to study the underlying mechanism(s) by analyzing protein expression levels of known cell cycle regulators. The rate of cell proliferation in mammalian cells is determined mainly in the G_1 phase of the cell cycle by the specific activation of cyclin-dependent kinases, which are in turn negatively regulated by two families of cyclin-dependent kinase inhibitors (CKIs) (66). First, we compared total bone marrow cell extracts from control *MxCre*-negative and in vivo deleted *Ring1B* (*MxCre* positive) mice. Western blot analysis showed increased levels of cyclin D2 (Fig. 4A) and also of the cell cycle progression indicator cyclin A (see Fig. S4A in the supplemental material) in extracts from *Ring1B*-deficient cells. Also, levels of the CKI p27 appeared slightly higher in mutant cells (see Fig. S4 in the supplemental material). However, the most prominent difference was observed for the levels of p16^{Ink4a}, another CKI which, while undetectable in extracts from nondeleted cells, gave a strong signal in *Ring1B*-deficient cell extracts (Fig. 4A). No signals were detected for cdc6, a component of the replication licensing machinery, the CKI p57, or p19^{Arf} in any of the extracts (see Fig. S4A in the supplemental material).

Since the most immature cells (i.e., HSCs and progenitors) represent only a minor contribution to total bone marrow cells, we performed Western blot analysis on mutant and control Lin$^-$ cells (Fig. 3B). In contrast to whole bone marrow, the expression pattern of cell cycle regulators in mutant Lin$^-$ cells showed an upregulation of proliferation activators cyclin D2

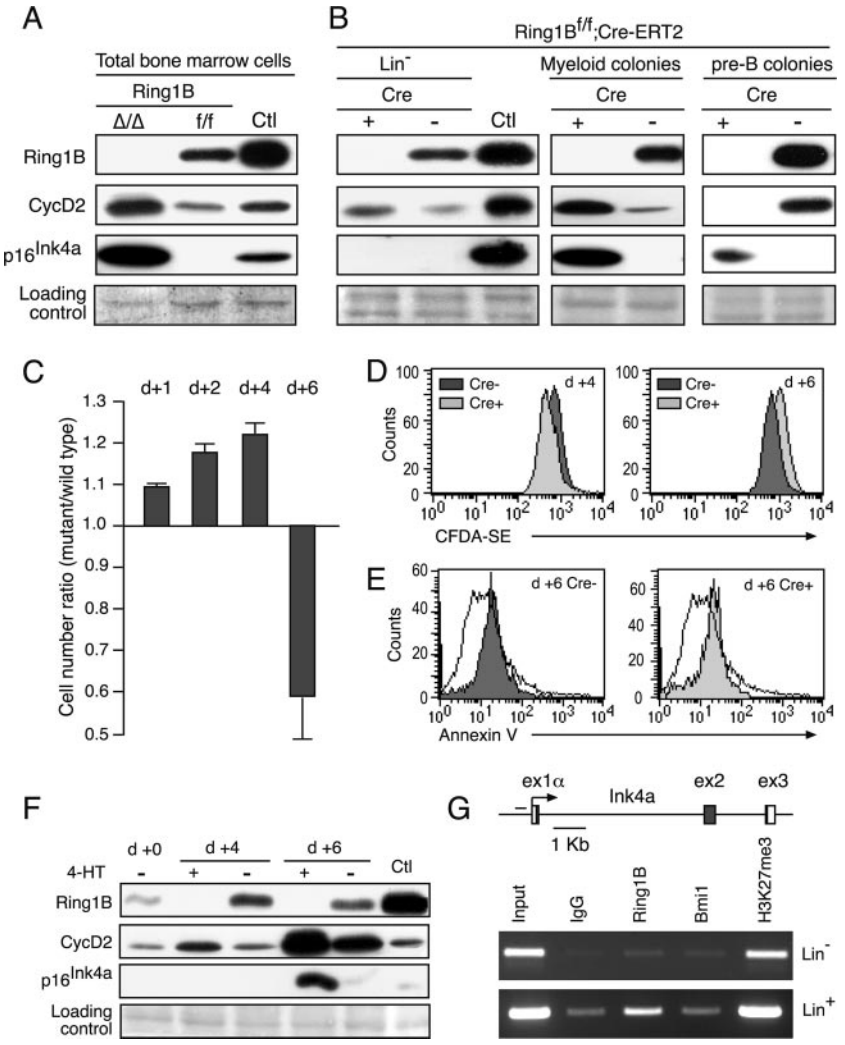

FIG. 4. Cell cycle regulator levels and proliferation rate are differentially affected by Ring1B along differentiation. (A and B) Representative Western blots (3 to 15 independent experiments) from the indicated extracts. (A) Bone marrow extracts from mice in which the *Ring1B* locus has been excised as a result of the expression of MxCre (Δ/Δ; Cre^+) and from *Ring1B*$^{f/f}$ (f/f; Cre^-) mice. (B) Blots at left are extracts from Lin^- cells immunomagnetically isolated from 4-HT-treated or untreated *Ring1B*$^{f/f}$; *Cre-ERT2* bone marrow cells cultured for 48 h. Blots of extracts from myeloid colonies harvested after culturing Lin^- cells for 8 days in methylcellulose medium without or with 4-HT are shown in the middle. At right are blots of extracts from pooled pre-B-cell colonies grown after 8-day cultures of *Ring1B*$^{f/f}$ and *Ring1B*-deficient bone marrow cells. Ctl, extracts from mouse erythroleukemia cells; +, with 4-HT treatment; −, without 4-HT treatment. In panels A and B, Ponceau red-stained membranes were used as a loading control. (C to F) Isolated Lin^- cells were cultured in suspension for the indicated times in differentiation medium containing stem cell factor, IL-3, and IL-6 in the presence (+) or absence (−) of 4-HT. (C) Differential accumulation of mutant and control cells with time in culture. Bars represent the average ratio of the percentage of mutant to control cells, considering the value of control cells as 1. (D) Switch in the values of CFDA-SE fluorescence of cells in cultures in which the *Ring1B* locus has been excised as a result of 4-HT treatment (Cre^+) and in untreated (nonexcised *Ring1B*; Cre^-) cultures at the indicated times. (E) FITC-conjugated annexin V labeling of propidium iodide-impermeable viable cells present in day +6 cells cultured with (right) or without (left) 4-HT. Overlaid empty histogram corresponds to cells treated under the same conditions but with no added annexin V. (F) Western blot analysis of cell extracts obtained from cells cultured in the presence (+) or the absence (−) of 4-HT for the indicated times. Day +0 corresponds to extracts of Lin^- cells isolated from the bone marrow of *Ring1B*$^{f/f}$; *Cre-ERT2* mice at the time of sacrifice. Controls and loading control are as described in panels A and B. (G) *Ink4a* promoter occupancy by Ring1B and Bmi1 in progenitors and maturing hematopoietic cells. At top is a schematic representation of the *p16*^{Ink4a} gene locus shows exons and coding (filled) sequences and the amplicon used for ChIP assays. Lin^- and Lin^+ cell populations were immunomagnetically isolated from bone marrow and chromatin analyzed using the indicated antibodies (bottom). Ex, exon; H3K27me3, trimethylated H3K27; IgG, immunoglobulin G; d, day.

(Fig. 4B, left), cyclin A, and cdc6 (see Fig. S4A in the supplemental material) with a concomitant absence of proliferation inhibitors $p16^{Ink4a}$ (Fig. 4B, left), p27, and p57 (see Fig. S4A in the supplemental material). However, the analysis of colonies harvested from Lin^- cell methylcellulose cultures at day 8 showed a sustained upregulation of cyclin D2 together with a dramatic increase of $p16^{Ink4a}$ levels in maturing *Ring1B*-deficient cells only (Fig. 4B, middle panel), thus resembling the expression pattern seen in unfractionated bone marrow cells. A similar upregulation of $p16^{Ink4a}$ levels was observed in extracts from cultured mutant pre-B cells (Fig. 4B, right). Only cyclin D3, which is needed for the expansion of pre-B cells

(13), was detected in these cells, and its expression was hardly affected by the lack of Ring1B in either pre-B cells or myeloid cells (see Fig. S4C in the supplemental material), suggesting that the effect on cyclin D2 is specific. Modest increases in p27 and p57 levels were also observed in maturing mutant cells (see Fig. S4B in the supplemental material). These data show that *Ring1B* inactivation alters the expression pattern of cell cycle regulators in differentiating cells and suggest that the resulting populations of mature and immature cells are endowed with reduced and enhanced proliferation rates, respectively.

We investigated these cell populations by using liquid cultures of ex vivo *Ring1B*-ablated Lin^- cells under conditions that recapitulate the differentiation events occurring in normal myelopoiesis. Initially after treatment, the relative accumulation of cells was faster in mutant (+4-HT; Cre^+) than in control (−4-HT; Cre^-) cultures (Fig. 4C). However, by day 6 after treatment, this ratio was inverted, and Ring1B-expressing cultures contained more cells than those of *Ring1B*-deficient cells. Analysis of CFDA-SE fluorescence decay confirmed the inversion of cell division rates between days 4 and 6 after 4-HT (Fig. 4D) treatment. The lower accumulation of mutant cells did not result from increased cell death, as determined by annexin V staining (Fig. 4E). Instead, the late upregulation of $p16^{Ink4a}$, detected only by day 6 after treatment (Fig. 4F), correlated with the switch in proliferation rate. This contrasted with the prompt upregulation of the proliferation promoter cyclin D2 in mutant cultures (Fig. 4F), which, in the absence of the inhibitor $p16^{Ink4a}$, would explain the enhanced proliferation observed before day +6. A possible explanation for the differential regulation of $p16^{Ink4a}$ in immature versus mature cells may be related to the decreasing levels of Bmi1 during hematopoietic differentiation (26), which would ensure $p16^{Ink4a}$ silencing in progenitors, even in the absence of Ring1B. We tested this by analyzing promoter occupancy at the *Ink4a* locus in ChIP assays and found that whereas Ring1B was detected in both immature Lin^- and maturing Lin^+ cells, Bmi1 was seen associated predominantly in the immature compartment (Fig. 4G).

Collectively, these results show that through the balanced expression of positive and negative cell cycle regulators, Ring1B controls the expansion of differentiating hematopoietic cells both by restricting proliferation of progenitors and by contributing to their expansion during maturation.

Ink4a deficiency rescues only the expansion defects of Ring1B-deficient hematopoietic cells. Given the correlation seen between $p16^{Ink4a}$ upregulation and proliferation inhibition in maturing ex vivo *Ring1B*-deleted cells, the overall decrease of bone marrow cells associated with *Ring1B* inactivation could be explained by similar mechanisms. To test this hypothesis, we crossed $Ring1B^{f/f}$; *MxCre* and $Ring1B^{f/f}$ mice with a mouse line carrying an *Ink4a* null mutation which does not express either $p16^{Ink4a}$ or $p19^{Arf}$ (65). Bone marrow analysis after pIpC-induced *Ring1B* ablation showed that inactivation of the *Ink4a* locus abolished the differences in cellularities of bone marrow and spleen observed in single *Ring1B*-deficient cells (Fig. 5A). Furthermore, the severe reduction of pre-B-cell colonies associated with *Ring1B* inactivation was not observed in cultures of bone marrow cells that were also deficient in *Ink4a*, which showed even a further increase in the number and size of pre-B-cell CFU (Fig. 5B). In contrast, the increased

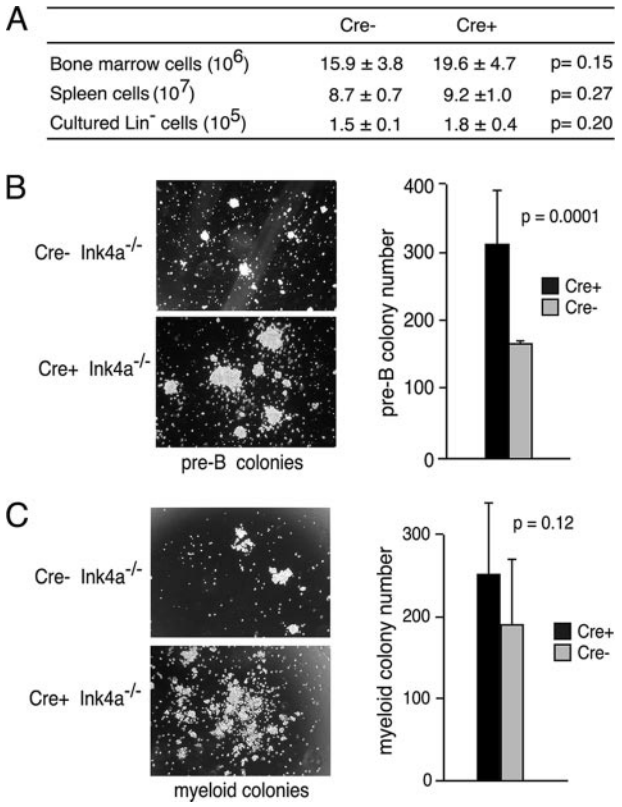

FIG. 5. *Ink4a* and *Ring1B* genetic interaction: *Ink4a* inactivation rescues impaired proliferation of *Ring1B*-deficient ($Ring1B^{\Delta/\Delta}$) maturing cells. (A) Total or fractionated Lin^- bone marrow and total spleen cell number from $Ring1B^{f/f}$; $Ink4a^{-/-}$ ($n = 6$) and $Ring1B^{\Delta/\Delta}$; $Ink4a^{-/-}$ ($n = 7$) mice. (B) Pre-B-cell colonies from $Ring1B^{f/f}$; $Ink4a^{-/-}$ and $Ring1B^{\Delta/\Delta}$; $Ink4a^{-/-}$ bone marrow cells. Photographs correspond to day +4 of culture and show the increased size and number of *Ink4a* mutant colonies and, in particular, of double mutant cultures. Histograms show pre-B-cell colony numbers at day +8 of culture. (C) Same experiment as in panel B but in myeloid clonogenic methylcellulose medium. Photographs were taken at day +8 of culture. Histograms depict total myeloid colony numbers in day +8 cultures.

number of *Ring1B*-deficient myeloid CFU was not affected by the lack of *Ink4a* (Fig. 5C), although the enlarged size of double mutant colonies indicated that *Ink4a* products could act by restricting the proliferative potential of maturing *Ring1B*-deficient cells. Since $p19^{Arf}$ is not affected by Ring1B inactivation, the results confirm that the proliferative deficits of *Ring1B*-deficient hematopoietic cells are due to the upregulation of $p16^{Ink4a}$ in maturing cells.

***Ring1B* deficiency results in an accelerated onset of hematopoietic neoplasias in the absence of *Ink4a*.** Mice with an inactive *Ink4a* locus spontaneously develop and succumb to a variety of tumors, mostly fibrosarcomas and lymphomas (62, 65). Remarkably, compound *Ring1B*; *Ink4a* mutant mice presented a quicker onset of fatal disease that lead to an acceleration of the death rate, on average 11 weeks after *Ring1B* ablation, as indicated in the survival plot shown in Fig. 6A. Four out of the six compound mutant mice which could be subjected to necropsy had developed splenomegalia and hepatomegalia (Fig. 6B, left), resulting from infiltration by cells which expressed the lymphoid marker Pax5 (Fig. 6E, right).

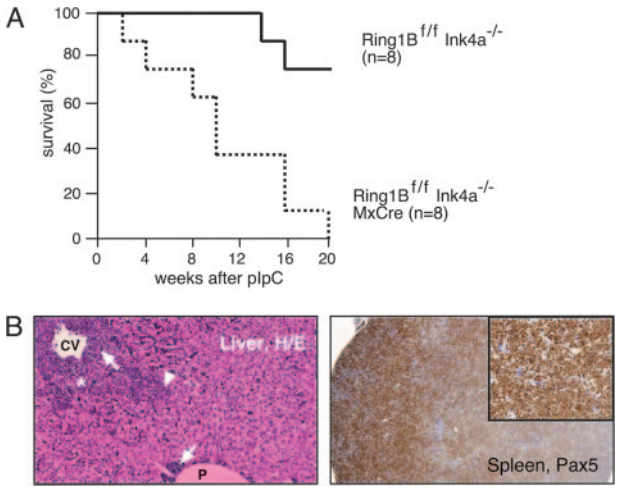

FIG. 6. Loss of Ring1B accelerates the onset of tumors associated to Ink4 inactivation. (A) Survival analysis of pIpC-injected *Ring1B*$^{f/f}$; *Ink4a*$^{-/-}$ ($n = 8$; solid lines) and *Ring1B*$^{f/f}$; *Ink4a*$^{-/-}$ *MxCre* ($n = 8$; dashed lines) mice. (B) Histochemical analysis of liver (left panel) and spleen (right panel) of a mouse in which the *Ring1B* and *Ink4a* loci are inactivated. Periportal (P) proliferation of tumor cells (arrows) with sinusoidal colonization in midzone areas (arrowhead) and marked distention of sinusoids (*) in the central vein (CV) area are shown. The normal architecture of the spleen is effaced by a diffuse proliferation of neoplastic cells. These tumor cells display positive immunostaining with Pax-5 antibody. H/E, hematoxylin and eosin stain.

The results show cooperation between the loss of function of a tumor suppressor (*Ink4a*) and the inactivation of *Ring1B*, which is in agreement with a role for *Ring1B* as a negative regulator of cell proliferation.

DISCUSSION

Elucidating the mechanisms underlying tissue self-renewal is important to understanding neoplastic processes. In this study, we provide genetic evidence supporting a distinctive role for the Polycomb protein Ring1B in the regulation of adult hematopoiesis. We find that Ring1B controls hematopoietic cell proliferation by acting as not only a positive regulator, as other PRC1 members, but also a negative regulator, depending on the maturational stage of cell differentiation. Thus, while restricting proliferation of early myeloid progenitors, Ring1B is needed for the expansion of maturing, cell lineage-committed precursors of both myeloid and lymphoid B-cell lineages. We demonstrate that these effects are mediated, at least in part, via downregulation of opposing cell cycle regulators, the G_1 cyclin D2 and its inhibitor p16^{Ink4a}.

Dual roles of Ring1B in positive and negative regulation of cell proliferation through downregulation of cell cycle inhibitors and activators. The hematopoietic compartment is among the tissues most affected by mutations in PcG genes, resulting in smaller thymi and spleens and a hypocellular bone marrow (36, 55). Inactivation of *Ring1B* results in a hematopoietic phenotype milder than that of other PRC1 mutant mice but equally consistent with a positive role in cell proliferation. However, the enlargement of the size of the mutant progenitor compartment indicates that Ring1B also acts as an antiproliferative regulator. The accumulation of *Ring1B*-deficient immature cells seems to be due mostly to their hyperproliferative phenotype rather than to reduced apoptosis or defective differentiation. Thus, the antiproliferative activity of Ring1B contrasts with the most prominent role of other PRC1 subunits as proliferation promoters, e.g., Bmi1. It also resembles that of the PRC2 component Eed, whose inactivation antagonizes the effects of a *Bmi1* mutation (35). Moreover, the use of an ex vivo inactivation model shows that these proliferative alterations are, at least in part, the result of *Ring1B* cell-autonomous regulated events.

In agreement with a dual role for Ring1B in negative and positive regulation of cell proliferation, we find that Ring1B targets both cell cycle activators and inhibitors. Usually, the activity of PcG proteins as promoters of cell proliferation is associated to their role as repressors of the *Ink4a* locus (23). We find that the inactivation of *Ring1B* also causes upregulation of p16^{Ink4a} but not of p19^{Arf}, similarly to the previous observation of *Ink4a* mRNA selective derepression in constitutively *Ring1B*-deficient mouse embryos (72). In addition, our analysis demonstrates that Ring1B regulates negatively the G_1 cyclin D2 and the replication factor cdc6, two characteristic promoters of cell proliferation.

Repression by PcG complexes usually refers to the mechanisms dealing with maintenance of transcriptionally silent loci. An example is the *Ink4a/Arf* locus, which is normally inactive in proliferating cells. Association of PcG components, including Ring1B, to genomic regions of *Ink4a/Arf* and its correlation with the repressed state are considered indications of direct transcriptional control (6, 21, 31). On the other hand, negative regulation of transcriptionally active loci, such as cyclin D2 in proliferating cells, appears as a novel scenario for Polycomb repression. However, studies in *Drosophila melanogaster* show that the *Cyclin A* gene, the product of which is needed for cell cycle progression, is repressed by PRC1 subunits, Polycomb and Polyhomeotic (42). Furthermore, Polycomb was found associated to the *Cyclin A* locus, just as Ring1B and Bmi1 appear bound to regions of the *Cyclin D2* gene in ES cells and fibroblasts (5, 7). It is likely, then, that the presence of Polycomb complexes in the proximity of regulatory regions of active loci (6, 8, 50) may serve a regulatory role for fine-tuning of the transcriptional response. Regardless of the underlying mechanism(s), the finding that Ring1B negatively regulates cyclin D2 reinforces the notion that the role of PcG complexes in cell proliferation includes the regulation of components of the machinery involved in cell cycle progression.

Selective regulation of hematopoietic cell proliferation by Ring1B and other PcG products. Normal hematopoiesis displays an orchestrated use of the cell cycle machinery components in order to ensure the self-renewal and expansion activities associated with the various stages of cell differentiation of hematopoietic lineages (53). These include proliferative responses as diverse as the high self-renewal capacity and low proliferative rate of HSCs, the various proliferation rates of their progeny along their maturation, or retrieval from active proliferation of fully differentiated cells (58).

In our studies, *Ring1B* inactivation resulted in upregulation of cyclin D2 in most hematopoietic cells analyzed, except for B-cell precursors, whereas that of p16^{Ink4a} was detected only in maturing B and myeloid cells but not in progenitors, thus providing an explanation for their altered proliferation rates.

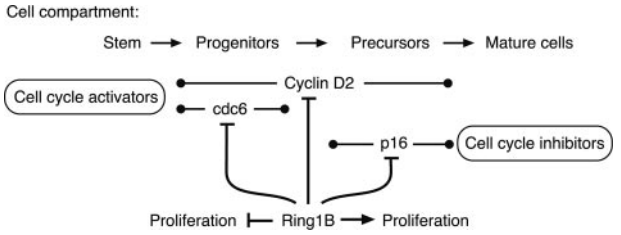

FIG. 7. Proposed model for Ring1B proliferation control during hematopoiesis. During normal hematopoiesis, Ring1B regulates progenitor and precursor cell expansion by controlling the balance between positive and negative proliferating signals. In *Ring1B*-deficient hematopoietic cells, proliferation activators cyclin D2 and cdc6 are upregulated in myeloid progenitors whereas the $p16^{Ink4a}$ proliferation inhibitor is upregulated only in more mature myeloid and lymphoid precursor cells. As a result, the early myeloid progenitor population is expanded whereas B-cell and myeloid maturing cell populations are reduced.

Mutant myeloid progenitor hyperproliferation would result from increased cyclin D2, in the absence of $p16^{Ink4a}$, as it occurs in *Cyclin D2*-transduced bone marrow cells (61). In turn, progressive accumulation of $p16^{Ink4a}$ along differentiation would abrogate the proliferative potential of the maturing progeny, despite their high content of cyclin D2, thereby resulting in a hypoplastic bone marrow. In this simple hypothesis, inhibition, but not promotion, of proliferation caused by *Ring1B* inactivation would be alleviated by loss of $p16^{Ink4a}$. Indeed, myeloid and B-cell precursors of mice bearing a coincident loss of *Ring1B* and *Ink4a* proliferate efficiently, and the reduced cellularity of *Ring1B*-deficient bone marrow is restored in the compound mutant. Instead, the hyperproliferative phenotype elicited by *Ring1B* inactivation in myeloid progenitors was not reversed by the absence of *Ink4a*. Altogether, our data support a broad regulatory role for Ring1B in the differentiation/expansion of adult hematopoietic cells by integrating signals during amplification of immature progenitors and during the expansion of their maturing progeny (Fig. 7).

The contrasting differences between hematopoietic alterations associated with Ring1B ablation and those seen in mice lacking some of their interacting partners in PRC1 complex(es), i.e., Bmi1, Mel18, M33, and Mbt1 (1, 14, 71), are likely a reflection of differential targeting in distinct cell types by complexes that vary in composition or activity. For instance, maintenance of repression of *Ink4a*/*Arf* in HSCs and early progenitors occurs in the absence of Ring1B but not in the absence of Bmi1 (48); another example is the p57 derepression in *Mbt1*-null myeloid progenitors (2). Given the increasing biochemical diversity of Ring1B-containing complexes (22, 47, 59), it appears that a definition of the expression pattern of their subunits throughout the differentiation stages of the various lineages will be needed for a comprehensive understanding of Polycomb complex function in hematopoiesis.

***Ring1B-Ink4a* interaction: implications for tumorigenesis.** The role of Ring1B as a proliferation promoter through repression of inhibitors of cell proliferation is consistent with the rescue of *Ring1B*-deficient bone marrow hypocellularity by *Ink4a*/*Arf* inactivation. This observation is reminiscent of the substantial restoration of the self-renewing capacity of HSCs (48) and of thymocytes and splenocytes of $Bmi1^{-/-}$ *Ink4a*/$Arf^{-/-}$ mice (9). Bmi1-mediated repression of *Ink4a* appears as a causal agent of primed cell proliferation in tumors, and protein expression analysis shows upregulation of Bmi1 in a variety of tumor cells. Similarly, Ring1B protein expression is increased in a variety of tumors (60), and its expression correlates with poor prognosis in a subset of malignant human cancers (24). However, the antiproliferative activity of Ring1B may also play a role in the development of neoplastic processes, as suggested by the decreased latency of tumor development in mice whose bone marrow is doubly *Ring1B* and *Ink4a*/*Arf* deficient compared to those lacking only *Ink4a*/*Arf*. Since *Ring1B* inactivation does not lead to $p19^{Arf}$ upregulation, the contribution of Ring1B in the absence of $p16^{Ink4a}$ to neoplastic events may lie in the presence of a population of progenitors with enhanced self-renewal properties susceptible of transformation (16, 32), thus cooperating with other genetic/epigenetic lesions appearing during the onset and development of tumors.

In conclusion, we have identified an antiproliferative role for Ring1B in the expansion of progenitor cells, mediated by the suppression of a positive regulator of the cell cycle machinery, which may be important in the tight control of proliferation occurring during adult hematopoiesis. It will be of interest to investigate whether this role in cell turnover takes place also in other self-renewing tissues.

ACKNOWLEDGMENTS

We thank Y. Mizutani and M. Iida for excellent technical help and T. Ikawa (RCAI) for help with quantitative PCR analysis. We thank V. Campuzano and M. Barbacid for the $RERT^{ert}$ mouse line, M. Serrano for the $Ink4^{-/-}$ mouse line, K. Helin for anti-Bmi1 antibody, M. Sánchez-Beato for assistance with immunohistochemistry, and D. Kioussis (NIMR) for critical reading of the manuscript.

T.M. and M.R-T. were recipients of FPI and FPU fellowships, respectively, from the Ministerio de Educación y Ciencia. This work was supported by grants from the Fundación Médica Mutua Madrileña (C.C.), Plan Nacional de Investigacion Científica BFU2005-03651 (C.C.) and SAF2004-06952-CO2-01 (M.V.), the OncoCycle program from the Comunidad de Madrid (M.V.), and in part by a grant of the Genome Network Project from the Ministry of Education Culture, Sports, Science and Technology of the Japanese Government (H.K.).

REFERENCES

1. **Akasaka, T., K. Tsuji, H. Kawahira, M. Kanno, K. Harigaya, L. Hu, Y. Ebihara, T. Nakahata, O. Tetsu, M. Taniguchi, and H. Koseki.** 1997. The role of *mel-18*, a mammalian Polycomb group gene, during IL-7-dependent proliferation of lymphocyte precursors. Immunity **7:**135–146.
2. **Arai, S., and T. Miyazaki.** 2005. Impaired maturation of myeloid progenitors in mice lacking novel Polycomb group protein MBT-1. EMBO. J. **24:**1863–1873.
3. **Atsuta, T., S. Fujimura, H. Moriya, M. Vidal, T. Akasaka, and H. Koseki.** 2001. Production of monoclonal antibodies against mammalian Ring1B proteins. Hybridoma **20:**43–46.
4. **Boyer, L. A., D. Mathur, and R. Jaenisch.** 2006. Molecular control of pluripotency. Curr. Opin. Genet. Dev. **16:**455–462.
5. **Boyer, L. A., K. Plath, J. Zeitlinger, T. Brambrink, L. A. Medeiros, T. I. Lee, S. S. Levine, M. Wernig, A. Tajonar, M. K. Ray, G. W. Bell, A. P. Otte, M. Vidal, D. K. Gifford, R. A. Young, and R. Jaenisch.** 2006. Polycomb complexes repress developmental regulators in murine embryonic stem cells. Nature **441:**349–353.
6. **Bracken, A. P., D. Kleine-Kohlbrecher, N. Dietrich, D. Pasini, G. Gargiulo, C. Beekman, K. Theilgaard-Mönch, S. Minucci, B. T. Porse, J. C. Marine, K. H. Hansen, and K. Helin.** 2007. The Polycomb group proteins bind throughout the INK4A-ARF locus and are disassociated in senescent cells. Genes Dev. **21:**525–530.
7. **Bracken, A. P., N. Dietrich, D. Pasini, K. H. Hansen, and K. Helin.** 2006. Genome-wide mapping of Polycomb target genes unravels their roles in cell fate transitions. Genes Dev. **20:**1123–1136.
8. **Breiling, A., L. P. O'Neill, D. D'Eliseo, B. M. Turner, and V. Orlando.** 2004.

Epigenome changes in active and inactive Polycomb-group-controlled regions. EMBO Rep. **5:**976–982.
9. **Bruggeman, S. W., M. E. Valk-Lingbeek, P. P. van der Stoop, J. J. Jacobs, K. Kieboom, E. Tanger, D. Hulsman, C. Leung, Y. Arsenijevic, S. Marino, and M. van Lohuizen.** 2005. Ink4a and Arf differentially affect cell proliferation and neural stem cell self-renewal in Bmi1-deficient mice. Genes Dev. **19:** 1438–1443.
10. **Buchwald, G., P. van der Stoop, O. Weichenrieder, A. Perrakis, M. van Lohuizen, and T. K. Sixma.** 2006. Structure and E3-ligase activity of the Ring-Ring complex of Polycomb proteins Bmi1 and Ring1b. EMBO J. **25:** 2465–2474.
11. **Buszczak, M., and A. C. Spradling.** 2006. Searching chromatin for stem cell identity. Cell **125:**233–236.
12. **Cao, R., L. Wang, H. Wang, L. Xia, H. Erdjument-Bromage, P. Tempst, R. S. Jones, and Y. Zhang.** 2002. Role of histone H3 lysine 27 methylation in Polycomb-group silencing. Science **298:**1039–1043.
13. **Cooper, A. B., C. M. Sawai, E. Sicinska, S. E. Powers, P. Sicinski, M. R. Clark, and I. Aifantis.** 2006. A unique function for cyclin D3 in early B cell development. Nat. Immunol. **7:**489–497.
14. **Coré, N., F. Joly, A. Boned, and M. Djabali.** 2004. Disruption of E2F signaling suppresses the INK4a-induced proliferative defect in M33-deficient mice. Oncogene **23:**7660–7668.
15. **Coré, N., S. Bel, S. J. Gaunt, M. Aurrand-Lions, J. Pearce, A. Fisher, and M. Djabali.** 1997. Altered cellular proliferation and mesoderm patterning in Polycomb-M33-deficient mice. Development **124:**721–729.
16. **Cozzio, A., E. Passegué, P. M. Ayton, H. Karsunky, M. L. Cleary, and I. L. Weissman.** 2003. Similar MLL-associated leukemias arising from self-renewing stem cells and short-lived myeloid progenitors. Genes Dev. **17:**3029–3035.
17. **Crosnier, C., D. Stamataki, and J. Lewis.** 2006. Organizing cell renewal in the intestine: stem cells, signals and combinatorial control. Nat. Rev. Genet. **7:**349–359.
18. **Czermin, B., R. Melfi, D. McCabe, V. Seitz, A. Imhof, and V. Pirrotta.** 2002. *Drosophila* enhancer of Zeste/ESC complexes have a histone H3 methyltransferase activity that marks chromosomal Polycomb sites. Cell **111:**185–196.
19. **del Mar Lorente, M., C. Marcos-Gutiérrez, C. Pérez, J. Schoorlemmer, A. Ramírez, T. Magin, and M. Vidal.** 2000. Loss- and gain-of-function mutations show a Polycomb group function for Ring1A in mice. Development **127:**5093–5100.
20. **de Napoles, M., J. E. Mermoud, R. Wakao, Y. A. Tang, M. Endoh, R. Appanah, T. B. Nesterova, J. Silva, A. P. Otte, M. Vidal, H. Koseki, and N. Brockdorff.** 2004. Polycomb group proteins Ring1A/B link ubiquitylation of histone H2A to heritable gene silencing and X inactivation. Dev. Cell **7:**663–676.
21. **Dietrich, N., A. P. Bracken, E. Trinh, C. K. Schjerling, H. Koseki, J. Rappsilber, K. Helin, and K. H. Hansen.** 2007. Bypass of senescence by the polycomb group protein CBX8 through direct binding to the INK4A-ARF locus. EMBO J. **26:**1637–1648.
22. **Gearhart, M. D., C. M. Corcoran, J. A. Wamstad, and V. J. Bardwell.** 2006. Polycomb group and SCF ubiquitin ligases are found in a novel BCOR complex that is recruited to BCL6 targets. Mol. Cell. Biol. **26:**6880–6889.
23. **Gil, J., and G. Peters.** 2006. Regulation of the INK4b-ARF-INK4a tumour suppressor locus: all for one or one for all. Nat. Rev. Mol. Cell Biol. **7:**667–677.
24. **Glinsky, G. V., O. Berezovska, and A. B. Glinskii.** 2005. Microarray analysis identifies a death-from-cancer signature predicting therapy failure in patients with multiple types of cancer. J. Clin. Investig. **115:**1503–1521.
25. **Hemenway, C. S., B. W. Halligan, and L. S. Levy.** 1998. The Bmi-1 oncoprotein interacts with dinG and MPh2: the role of RING finger domains. Oncogene **16:**2541–2547.
26. **Hosen, N., T. Yamane, M. Muijtjens, K. Pham, M. F. Clarke, and I. L. Weissman.** 2007. Bmi-1-green fluorescent protein-knock-in mice reveal the dynamic regulation of bmi-1 expression in normal and leukemic hematopoietic cells. Stem Cells **25:**1635–1644.
27. **Jacobs, J. J., B. Scheijen, J. W. Voncken, K. Kieboom, A. Berns, and M. van Lohuizen.** 1999. Bmi-1 collaborates with c-Myc in tumorigenesis by inhibiting c-Myc-induced apoptosis via INK4a/ARF. Genes Dev. **13:**2678–2690.
28. **Kajiume, T., Y. Ninomiya, H. Ishihara, R. Kanno, and M. Kanno.** 2004. Polycomb group gene mel-18 modulates the self-renewal activity and cell cycle status of hematopoietic stem cells. Exp. Hematol. **32:**571–578.
29. **Kato, Y., H. Koseki, M. Vidal, H. Nakauchi, and A. Iwama.** 2007. Unique composition of polycomb repressive complex 1 in hematopoietic stem cells. Int. J. Hematol. **85:**179–181.
30. **Kondo, M., I. L. Weissman, and K. Akashi.** 1997. Identification of clonogenic common lymphoid progenitors in mouse bone marrow. Cell **91:**661–672.
31. **Kotake, Y., R. Cao, P. Viatour, J. Sage, Y. Zhang, and Y. Xiong.** 2007. pRB family proteins are required for H3K27 trimethylation and Polycomb repression complexes binding to and silencing $p16^{INK4a}$ tumor suppressor gene. Genes Dev. **21:**49–54.
32. **Krivtsov, A. V., D. Twomey, Z. Feng, M. C. Stubbs, Y. Wang, J. Faber, J. E. Levine, J. Wang, W. C. Hahn, D. G. Gilliland, T. R. Golub, and S. A. Armstrong.** 2006. Transformation from committed progenitor to leukaemia stem cell initiated by MLL-AF9. Nature **442:**818–822.
33. **Kühn, R., F. Schwenk, M. Aguet, and K. Rajewsky.** 1995. Inducible gene targeting in mice. Science **269:**1427–1429.
34. **Kuzmichev, A., K. Nishioka, H. Erdjument-Bromage, P. Tempst, and D. Reinberg.** 2002. Histone methyltransferase activity associated with a human multiprotein complex containing the Enhancer of Zeste protein. Genes Dev. **16:**2893–2905.
35. **Lessard, J., A. Schumacher, U. Thorsteinsdottir, M. van Lohuizen, T. Magnuson, and G. Sauvageau.** 1999. Functional antagonism of the Polycomb-group genes Eed and Bmi1 in hemopoietic cell proliferation. Genes Dev. **13:**2691–2703.
36. **Lessard, J., and G. Sauvageau.** 2003. Polycomb group genes as epigenetic regulators of normal and leukemic hemopoiesis. Exp. Hematol. **31:**567–585.
37. **Lessard, J., and G. Sauvageau.** 2003. Bmi-1 determines the proliferative capacity of normal and leukaemic stem cells. Nature **423:**255–260.
38. **Leung, C., M. Lingbeek, O. Shakhova, J. Liu, E. Tanger, P. Saremaslani, M. Van Lohuizen, and S. Marino.** 2004. Bmi1 is essential for cerebellar development and is overexpressed in human medulloblastomas. Nature **428:**337–341.
39. **Levine, S. S., A. Weiss, H. Erdjument-Bromage, Z. Shao, P. Tempst, and R. E. Kingston.** 2002. The core of the Polycomb repressive complex is compositionally and functionally conserved in flies and humans. Mol. Cell. Biol. **22:**6070–6078.
40. **Levine, S. S., I. F. King, and R. E. Kingston.** 2004. Division of labor in Polycomb group repression. Trends Biochem. Sci. **29:**478–485.
41. **Martinez, A. M., and G. Cavalli.** 2006. The role of Polycomb group proteins in cell cycle regulation during development. Cell Cycle **5:**1189–1197.
42. **Martinez, A. M., S. Colomb, J. Déjardin, F. Bantignies, and G. Cavalli.** 2006. Polycomb group-dependent cyclin A repression in *Drosophila*. Genes. Dev. **20:**501–513.
43. **Mijimolle, N., J. Velasco, P. Dubus, C. Guerra, C. A. Weinbaum, P. J. Casey, V. Campuzano, and M. Barbacid.** 2005. Protein farnesyltransferase in embryogenesis, adult homeostasis, and tumor development. Cancer Cell **7:**313–324.
44. **Molofsky, A. V., R. Pardal, T. Iwashita, I. K. Park, M. F. Clarke, and S. J. Morrison.** 2003. Bmi-1 dependence distinguishes neural stem cell self-renewal from progenitor proliferation. Nature **425:**962–967.
45. **Molofsky, A. V., S. He, M. Bydon, S. J. Morrison, and R. Pardal.** 2005. Bmi-1 promotes neural stem cell self-renewal and neural development but not mouse growth and survival by repressing the $p16^{Ink4a}$ and $p19^{Arf}$ senescence pathways. Genes Dev. **19:**1432–1437.
46. **Müller, J., C. M. Hart, N. J. Francis, M. L. Vargas, A. Sengupta, B. Wild, E. L. Miller, M. B. O'Connor, R. E. Kingston, and J. A. Simon.** 2002. Histone methyltransferase activity of a *Drosophila* Polycomb group repressor complex. Cell **111:**197–208.
47. **Ogawa, H., K. Ishiguro, S. Gaubatz, D. M. Livingston, and Y. Nakatani.** 2002. A complex with chromatin modifiers that occupies E2F- and Myc-responsive genes in G0 cells. Science **296:**1132–1136.
48. **Oguro, H., A. Iwama, Y. Morita, T. Kamijo, M. van Lohuizen, and H. Nakauchi.** 2006. Differential impact of Ink4a and Arf on hematopoietic stem cells and their bone marrow microenvironment in Bmi1-deficient mice. J. Exp. Med. **203:**2247–2253.
49. **Ohta, H., A. Sawada, J. Y. Kim, S. Tokimasa, S. Nishiguchi, R. K. Humphries, J. Hara, and Y. Takihara.** 2002. Polycomb group gene rae28 is required for sustaining activity of hematopoietic stem cells. J. Exp. Med. **195:**759–770.
50. **Papp, B., and J. Müller.** 2006. Histone trimethylation and the maintenance of transcriptional ON and OFF states by TrxG and PcG proteins. Genes. Dev. **20:**2041–2054.
51. **Park, I. K., D. Qian, M. Kiel, M. W. Becker, M. Pihalja, I. L. Weissman, S. J. Morrison, and M. F. Clarke.** 2003. Bmi-1 is required for maintenance of adult self-renewing haematopoietic stem cells. Nature **423:**302–305.
52. **Pasini, D., A. P. Bracken, and K. Helin.** 2004. Polycomb group proteins in cell cycle progression and cancer. Cell Cycle **3:**396–400.
53. **Passegué, E., A. J. Wagers, S. Giuriato, W. C. Anderson, and I. L. Weissman.** 2005. Global analysis of proliferation and cell cycle gene expression in the regulation of hematopoietic stem and progenitor cell fates. J. Exp. Med. **202:**1599–1611.
54. **Raaphorst, F. M.** 2005. Deregulated expression of Polycomb-group oncogenes in human malignant lymphomas and epithelial tumors. Hum. Mol. Genet. **14**(Suppl. 1)**:**R93–R100.
55. **Raaphorst, F. M., A. P. Otte, and C. J. Meijer.** 2001. Polycomb-group genes as regulators of mammalian lymphopoiesis. Trends Immunol. **22:**682–690.
56. **Rando, T. A.** 2006. Stem cells, ageing and the quest for immortality. Nature **441:**1080–1086.
57. **Ringrose, L., and R. Paro.** 2004. Epigenetic regulation of cellular memory by the polycomb and trithorax group proteins. Annu. Rev. Genet. **38:**413–443.
58. **Rosenbauer, F., and D. G. Tenen.** 2007. Transcription factors in myeloid development: balancing differentiation with transformation. Nat. Rev. Immunol. **7:**105–117.
59. **Sánchez, C., I. Sánchez, J. A. Demmers, P. Rodriguez, J. Strouboulis, and M.**

Vidal. 2007. Proteomic analysis of Ring1B/Rnf2 interactors identifies a novel complex with the Fbxl10/ Jmjd1B histone demethylase and the BcoR corepressor. Mol. Cell. Proteomics **6:**820–834.
60. **Sánchez-Beato, M., E. Sánchez, J. González-Carreró, M. Morente, A. Díez, L. Sánchez-Verde, M. C. Martín, J. C. Cigudosa, M. Vidal, and M. A. Piris.** 2006. Variability in the expression of polycomb proteins in different normal and tumoral tissues. A pilot study using tissue microarrays. Mod. Pathol. **19:**684–694.
61. **Sasaki, Y., C. T. Jensen, S. Karlsson, and S. E. Jacobsen.** 2004. Enforced expression of cyclin D2 enhances the proliferative potential of myeloid progenitors, accelerates in vivo myeloid reconstitution, and promotes rescue of mice from lethal myeloablation. Blood **104:**986–992.
62. **Schmitt, C. A., M. E. McCurrach, E. de Stanchina, R. R. Wallace-Brodeur, and S. W. Lowe.** 1999. INK4a/ARF mutations accelerate lymphomagenesis and promote chemoresistance by disabling p53. Genes. Dev. **13:**2670–2677.
63. **Schoorlemmer, J., C. Marcos-Gutiérrez, F. Were, R. Martínez, E. García, D. P. Satijn, A. P. Otte, and M. Vidal.** 1997. Ring1A is a transcriptional repressor that interacts with the Polycomb-M33 protein and is expressed at rhombomere boundaries in the mouse hindbrain. EMBO J. **16:**5930–5942.
64. **Schuettengruber, B., D. Chourrout, M. Vervoort, B. Leblanc, and G. Cavalli.** 2007. Genome regulation by polycomb and trithorax proteins. Cell **128:**735–745.
65. **Serrano, M., H. Lee, L. Chin, C. Cordon-Cardo, D. Beach, and R. A. DePinho.** 1996. Role of the INK4a locus in tumor suppression and cell mortality. Cell **85:**27–37.
66. **Sherr, C. J., and J. M. Roberts.** 1999. CDK inhibitors: positive and negative regulators of G1-phase progression. Genes Dev. **13:**1501–1512.
67. **Soriano, P.** 1997. The PDGF alpha receptor is required for neural crest cell development and for normal patterning of the somites. Development **124:**2691–2700.
68. **Sparmann, A., and M. van Lohuizen.** 2006. Polycomb silencers control cell fate, development and cancer. Nat. Rev. Cancer. **6:**846–856.
69. **Takihara, Y., D. Tomotsune, M. Shirai, Y. Katoh-Fukui, K. Nishii, M. A. Motaleb, M. Nomura, R. Tsuchiya, Y. Fujita, Y. Shibata, T. Higashinakagawa, and K. Shimada.** 1997. Targeted disruption of the mouse homologue of the *Drosophila* polyhomeotic gene leads to altered anteroposterior patterning and neural crest defects. Development **124:**3673–3682.
70. **Tokimasa, S., H. Ohta, A. Sawada, Y. Matsuda, J. Y. Kim, S. Nishiguchi, J. Hara, and Y. Takihara.** 2001. Lack of the Polycomb-group gene rae28 causes maturation arrest at the early B-cell developmental stage. Exp. Hematol. **29:**93–103.
71. **van der Lugt, N. M., J. Domen, K. Linders, M. van Roon, E. Robanus-Maandag, H. te Riele, M. van der Valk, J. Deschamps, M. Sofroniew, and M. van Lohuizen.** 1994. Posterior transformation, neurological abnormalities, and severe hematopoietic defects in mice with a targeted deletion of the *bmi-1* proto-oncogene. Genes Dev. **8:**757–769.
72. **Voncken, J. W., B. A. Roelen, M. Roefs, S. de Vries, E. Verhoeven, S. Marino, J. Deschamps, and M. van Lohuizen.** 2003. Rnf2 (Ring1b) deficiency causes gastrulation arrest and cell cycle inhibition. Proc. Natl. Acad. Sci. USA **100:**2468–2473.
73. **Wang, H., L. Wang, H. Erdjument-Bromage, M. Vidal, P. Tempst, R. S. Jones, and Y. Zhang.** 2004. Role of histone H2A ubiquitination in Polycomb silencing. Nature **431:**873–878.
74. **Weissman, I. L.** 2000. Stem cells: units of development, units of regeneration, and units in evolution. Cell **100:**157–168.